



POLITECNICO
MILANO 1863

DIPARTIMENTO DI MECCANICA



Innovative metallic solutions for alpine ski bases

Ripamonti, Francesco; Furlan, Valentina; Demir, Ali G.; Previtali, Barbara; Derai, Michele; Cheli, Federico; Ossi, Paolo M.

This article may be downloaded for personal use only. Any other use requires prior permission of the author and AIP Publishing. This article appeared in Ripamonti, F., Furlan, V., Demir, A.G., Previtali, B., Derai, M., Cheli, F., Ossi, P.M. Innovative metallic solutions for alpine ski bases (2018) Journal of Vacuum Science and Technology B: Nanotechnology and Microelectronics, 36 (1), art. no. 01A108, and may be found at <http://dx.doi.org/10.1116/1.5002542>

This content is provided under [CC BY-NC-ND 4.0](https://creativecommons.org/licenses/by-nc-nd/4.0/) license



Innovative Metallic Solutions for Alpine Ski Bases

Francesco Ripamonti ^{a)}, Valentina Furlan, Ali G. Demir, Barbara Previtali,
Michele Derai, Federico Cheli

Department of Mechanical Engineering, Politecnico di Milano, Via La Masa 1, 20156 Milan, Italy

Paolo M. Ossi

Department of Energy, Politecnico di Milano, Via Ponzio 34-3, 20133 Milan, Italy

^{a)} Electronic mail: francesco.ripamonti@polimi.it

Abstract

Ski manufacturers are interested in improving the ski performances in terms of fast sliding, excellent trajectory control and reduced maintenance. A possible approach to achieve this target is based on the substitution of the base material, moving from standard UHMWPE (Ultra High Molecular Weight Polyethylene) to metallic solutions. However, metallic materials, despite elevated mechanical properties, show a poor sliding behaviour, at least in their original condition. Although the interaction between ski base and snow is still an open field, we investigated the relationship between ice friction and material hydrophobicity. The wettability behaviour of surfaces can be managed by surface patterning. Among different techniques, Laser Surface Texturing (LST) is a promising method, which permits to modify surface features from the micrometre to millimetre scale, and it is attractive for an extension to industrial application.

In this work, the tribological properties of two metallic materials are investigated and a process to reduce the sliding friction against snow is proposed. LST is used in order to realize dimple patterning on metallic surfaces. Laser parameters are managed in order to control the dimple geometry and surface wettability using untreated substrates as reference conditions. A characterization with a prototype snow tribometer was performed determining friction coefficient and sliding performance of the laser treated metallic surfaces.

I. INTRODUCTION

Among technology products sports equipment are subjected to most relevant innovation. Considering a ski for alpine skiing, it has to demonstrate the capability of easy and controlled direction change, vibration damping, considerable bending stiffness, high torsion rigidity, low friction against snow and, if possible, low weight. The most recent innovation in the ski-manufacturing field is the carving, which dates back to the '90s. Since then, no innovation regarding the use of different materials of surface structures has been observed in the manufacturing of conventional skis. Nowadays, ski producers are interested in new solutions in order to improve ski performance and maintenance. Focusing on ski base, our starting point is the concept of a new ski structure breakthrough based on innovative metallic base. Metallic materials, like stainless steel or aluminium, have better mechanical properties than UHMWPE, which is the only material used for ski base manufacturing. The use of metallic materials would permit a reduction of the number of layers that constitute the ski structure, as well as the removal of the ski edges. In fact, a metallic ski base, once suitably shaped and sharpened

on the edges, substitutes for the usual low carbon steel edges, presently used. On the other hand, metallic materials present worse performances in terms of friction coefficient in contact with snow and ice, as compared to properly waxed UHMWPE. For this reason, in order to exploit the advantages of metallic materials, the friction behaviour of metallic materials on snow and ice should be improved.

Concerning the ice friction, Kietzig et al. described different states that are involved, where the water passes from solid to liquid throughout the interaction. Moving from an ice-solid interaction (without any lubrication) to a condition with a consistent layer of liquid, it is possible to identify four main states¹:

- i) dry friction
- ii) boundary lubrication
- iii) mixed friction
- iv) hydrodynamic lubrication.

The lower values of friction coefficient are achieved by boundary lubrication and mixed friction¹. The parameters of relevance when we consider the friction occurring in an ice/solid system were identified as temperature¹⁻³, speed^{1,2,4}, normal force^{1,4,5}, apparent contact area^{1,5,6}, roughness^{6,7}, superficial structure^{6,7}, wettability^{7,8}, icephobicity^{7,8}, relative humidity¹ and thermal conductivity⁹. Considering ski applications, temperature, speed, normal force, apparent contact area, relative humidity and thermal conductivity are difficult to be managed. On the other hand, surface structure, roughness, wettability, and icephobicity are correlated factors.

A change in surface morphology can be used in order to tune the surface response in terms of wettability and icephobicity. Surface modifications can be realized by different

methods. Among them, Laser Surface Texturing (LST) is a promising and flexible method to introduce changes in surface morphology at different dimension scales, ranging from millimetre to sub-micrometre. Moreover, the LST process can be adapted to be used in industrial large-scale production.

In the most common case, the laser beam can be used to generate a micrometric surface pattern changing the surface morphology and roughness. The surface texture geometry, dimension, and periodicity has a direct impact on the surface wettability¹⁰⁻¹². Hydrophobicity, in particular, permits to repel water from the surface¹³. Thus controlling the wettability of a solid surface can be used in order to predict its friction against ice^{7,8}.

Actually, another key feature characterizing a surface with low friction against ice or snow is icephobia. Icephobia concerns the ability of a surface both to prevent icing of the water that condenses or flows over it, and to ensure low adhesion force in the case ice possibly formed. In turn, icephobicity is correlated to the water wettability and hence is affected by the surface morphology and roughness.

Kietzig et al.¹ showed that it is possible to turn into superhydrophobic a metal surface by generating an ordered surface roughness by laser processing, leading to a lowering of the friction coefficient. The effect is more evident near the ice melting point where the film of liquid water between the contacting surfaces becomes thicker. Concerning icephobicity, Susoff et al.⁷ observed that an increase of surface roughness leads to an increment in the adhesion strength of ice on the surface. Bharathidasan et al.⁸ confirmed this result and reported that hydrophobic materials show an icephobic behaviour more pronounced than superhydrophobic ones. Therefore, despite a strong correlation

between the two behaviours, maximizing the contact angle does not necessarily correspond to an increased icephobicity, and the effect of surface texture should be assessed as a whole. The requirement of a low friction coefficient on ice is investigated in application fields ranging from aerospace to naval¹⁴⁻¹⁶, yet there is an evident lack of data concerning competitive winter sports^{17,18}.

In this work, we discuss the effect of different surface textures on innovative metallic ski bases. In particular, stainless steel and an aluminium alloy have been tested both in “untreated” and in “laser surface textured” conditions. Morphology and water contact angle were assessed. Finally, the performance of these solutions was characterized with a custom-built snow tribometer, able to operate under controlled temperature and humidity conditions. The tangential force between the materials and the snow surface was measured and a friction coefficient model was evaluated.

II. EXPERIMENTAL RESULTS

A. Materials

Two metallic materials were tested along with the more conventional ski material UHMWPE (Ultra High Molecular Weight Polyethylene). AISI 301 stainless steel was selected both for its excellent mechanical characteristics and for its good resistance to corrosion in an aqueous environment. The specimens were cold-rolled to 0.5 mm thickness. A commercial Al-alloy, namely Titanal®, a low-density metal already employed in ski manufacturing, was also chosen. Specimens with 0.4 mm thickness were used in the case of Titanal. Nominal compositions and mechanical properties of the two materials are reported in Table 1, Table 2 and Table 3.

Table 1 AISI 301 chemical composition (data from Lamina S.p.A.)

AISI 301	C%	Mn%	P%	S%	Si%	Cr%	Ni%	N%
	0.15	2.00	0.0045	0.030	0.75	16.00-18.00	6.00-8.00	0.10

Table 2 Titanal® chemical composition (data from AMAG_Austria Metal AG)

Titanal®	Al%	Cu%	Mg%	Zn%	Zr%
	88.7	1.7	2.5	7	0.1

Table 3 Mechanical properties relevant to ski bases for UHMWPE, AISI 301 and Titanal® (data from Lamina S.p.A. and AMAG_Austria Metal AG)

Material	Brinell hardness, HB [-]	Tensile strength [MPa]	Yield stress [MPa]
UHMWPE	40	48	21
AISI 301	588	1802	1613
Titanal®	207	630	580

B. Surface treatment design and patterning

It is worth to consider that UHMWPE and pristine Titanal bases were prepared with an imprint (a typical procedure adopted by ski-men, similar to a surface multi-directional scratch), applied thanks to the low hardness of both materials (compatible with their machinability).

Then, for the LST solutions, the adopted surface features are dimples, consisting in shallow blind holes with low aspect ratio. The use of dimpled surfaces in the study of snow and ice friction was not been widely investigated. However, dimples have been shown to improve

the tribological behaviour of mechanical components. Applied to mechanical surfaces, they can reduce the friction coefficient by acting as lubricant reservoirs, they contribute to load bearing by the generated hydrostatic pressure, and they reduce third body wear by entrapping the wear debris^{19,20}. Moreover, they are symmetric features that allow for avoiding directionality in this initial attempt to check the feasibility of surface texture to improve the ski performance. Indeed, for a surface that undergoes friction along a single direction the feature shape can be easily further optimized²¹.

Dimples can also have an impact on the surface wettability. The reduction of contact area and the fact that high capillary forces are required to fill in the cavities may rise the static contact angles²². However, compared to nanometric and hierarchical nano/micrometric surface structures, the change in wettability is limited¹⁰.

A further important factor is the simplicity offered by the dimple geometry. Compared to more complex nanometric features, such as Laser Induced Periodic Surface Structures (LIPSS) achieved with fs-pulsed lasers, dimpling with ns-pulsed lasers provides higher productivity.

Dimple diameter (d) and depth (h) are controlled via the laser percussion micro-drilling process, whereas the dimple spatial distribution is defined by the positioning of the laser beam by the scanner head. In this work, the dimples were realized with a fixed pitch (p) both in the horizontal and vertical directions. An industrial nanosecond fibre laser source (IPG Photonics YLP 1/100/50/50) was used to realize the texture. Beam handling was performed using a scanner head (TSH 8310 by Sunny Technology, Beijing, China) equipped with a f-theta lens having 100 mm focal length, obtaining a minimum beam spot diameter (d_0) of 39 μm . A point-by-point laser percussion drilling strategy realized

dimples²³. Process parameters were fixed in order to obtain the desired pattern in terms of diameter and depth, on the two different metals. Dimple characteristics are reported in Table 4. Figure 1 shows representative focus variation microscopy pictures of the laser textured metallic surfaces, prepared according to the parameter values in Table 4.

Table 4 Process parameters and average geometric properties of dimples realized on AISI 301 and Titanal®

Parameter	AISI 301	Titanal®
Pump current, PI% [%]	100	100
Pulse repetition rate , PRR [kHz]	50	50
Modulation time, t_{mod} [μ s]	70	70
Dimple diameter, D [μ m]	35 ± 3	43 ± 1
Dimple depth, h [μ m]	15 ± 3	38 ± 5

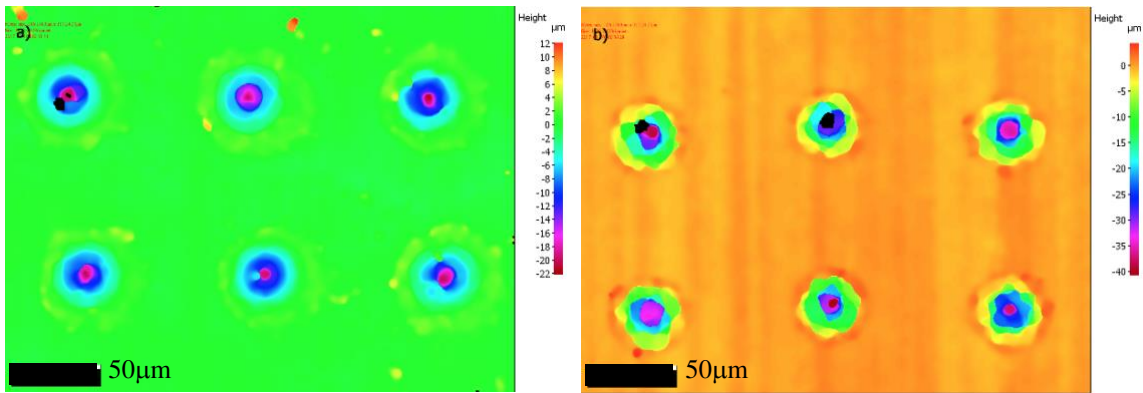


Figure 1 (Color Online) Focus variation microscopy pictures of the dimpled surfaces on a) AISI 301 and b) Titanal®

Water contact angles were measured with a sessile drop system using 2 μ l distilled water²⁴. The realized patterns provided the means for altering the water contact angle. Figure 2 shows the contact angle measurements of the metallic surfaces before (pristine) and after

LST. We notice that before texturing both of the materials are characterized by a hydrophilic behaviour ($CA < 90^\circ$) with average contact angles around 75° . The preparation of dimples led to an increase in the contact angle values, displacing the average values into the hydrophobic region ($CA > 90^\circ$), with average values about 110° for AISI 301 and 120° for Titanal. Such an increase can be interpreted in terms of entrapment within the dimples of the air that sustains the water droplet above the metal surface²².

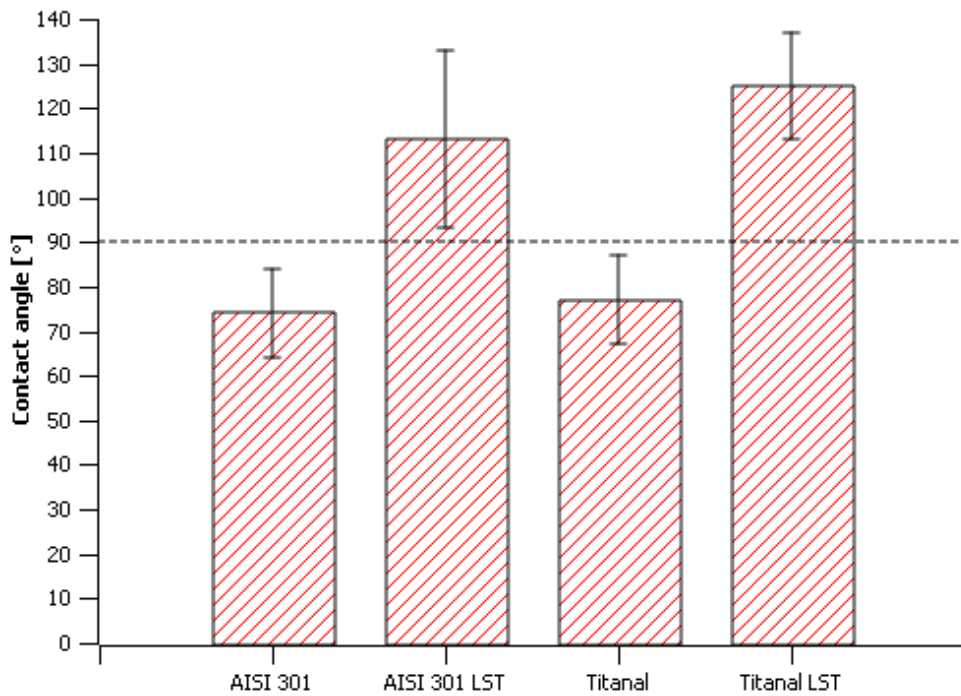


Figure 2 (Color Online) Comparison between contact angles of pristine and textured surfaces for AISI 301 and Titanal®

C. Evaluation of friction coefficient against snow

1. Design of a custom-built snow tribometer

To characterize the tribological behaviour of the samples, a snow tribometer was developed. To ensure no melting of the snow, tribometer was positioned in a climatic chamber (Binder, model MKF720) allowing for temperatures between +180°C and -40°C (Figure 3a). The temperature is controlled by a Pt100 sensor with a maximum fluctuation of $\pm 0.5^\circ\text{C}$ with respect to the setpoint. Ambient humidity is also controlled and monitored via a hygrometer (humidity range from 10% to 98% RH). The tests discussed here were all conducted at -10°C , with relative humidity 50%.

The tribometer is based on a rotating snow bed and a stationary sample holder. Inside a circular plate of aluminium (400 mm in diameter and 100 mm in height) a circular seat adapted to contain the snow was formed. The plate was keyed via a shaft and a bushing to a 250 W electric motor. The engine is connected to the tribometer frame by means of an aluminium cylindrical support by means of two roller bearings. These are sized in order to have a minimum resistance opposing to the force provided by the motor to rotate the plate. On the top plate, two rectangular supports are mounted. Such supports sustain two rails on which a carriage runs retaining the sample holder. The sample holder is made of ABS and shaped to simulate the tip of a ski. A 1.6 mm deep pocket with 50x50 mm² section was realized to insert the ski bases to be tested. The tested ski bases are attached to the pocket of the sample holder by means of a double-sided tape. In order to measure the tangential force, the sample holder is connected to a load cell (AEP transducers) with a nominal load of 10 N and a nominal sensibility of 2 mV/V. The electric motor is connected to a controller for the rotation speed regulation.

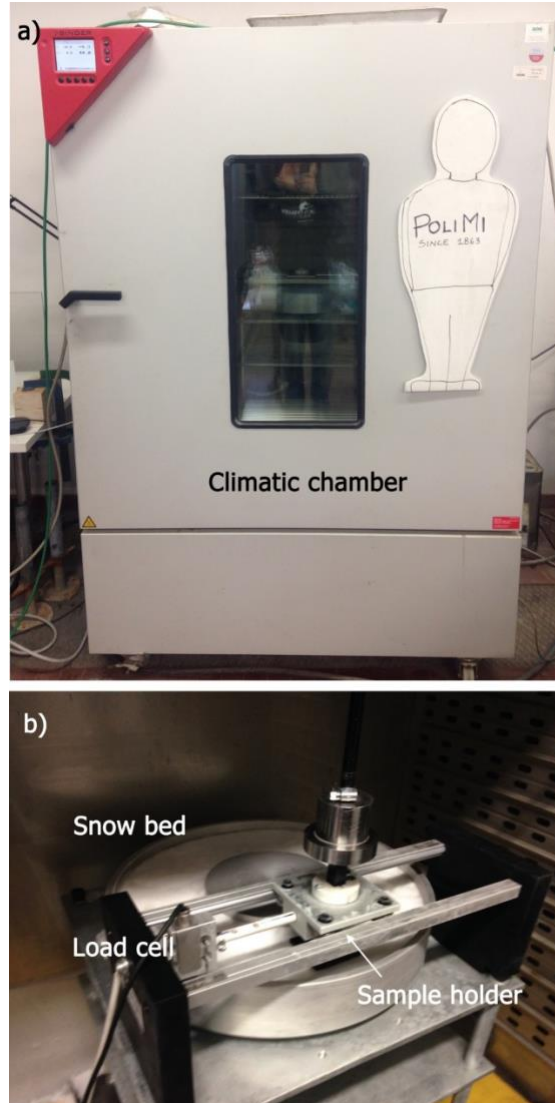


Figure 3 (Color Online) a) The custom build snow tribometer positioned in a climatic chamber. b) Details of the experimental setup

By starting the electric motor, the rotation produces a tangential friction force between the snow bed and the test specimen. Such a force is measured by the load cell connected to the sample holder. Figure 3b shows the experimental arrangement.

2. Test conditions

Five different samples, corresponding to different choices of material and surface treatment, were prepared and tested. Each sample was tested three times, resulting in a total number of 15 different tests. In Table 5 the tested samples are reported.

Table 5 Tested base materials and related surface treatments.

Sample Material	UHMWPE	AISI 301	Titanal®
Treatment	Waxed	Pristine	Pristine
		Laser Textured	Laser Textured
Sample thickness [mm]	1.6	0.5	0.4

A key point in tribological testing against snow is the management of temperature and snow conditions throughout the tests. Testing 15 samples as a function of different rotational speeds requires a careful planning to take into account the possible changes of snow track conditions. A preliminary campaign of tests was conducted to check the conditions of snow most suited to guarantee the repeatability of the measurements. The snow bed has to be carefully prepared by packing natural snow and partly icing it, thus approaching the conditions of a slope prepared for a high-level competition (consisting of packed, icy snow). Under such conditions, it was possible to perform an acceptable number of reliable tests before holes were accidentally formed by the sample along the track. Indeed, whenever the track loses its flatness, the test has to be stopped and the track has to be restored.

Each test was performed with a staircase increase of the rotational speed from 100 to 1000 rpm (Table 6). At each rotational speed, a permanence stage of 40 s was set to establish

steady track conditions and thus steady conditions in terms of the registered tangential force.

Table 6 Adopted motor rotation speeds for the snow tribometer tests

Parameter	Value
Snow plate rotational speed [rpm]	100-200-300-400-500-600-800-1000

In Figure 4 representative example of force measurements is reported. Each specimen was tested by applying 5 consecutive runs. In between each run the tribometer was stopped. By the end of the 5 runs a new specimen was mounted. Before starting a new set of runs the temperature and the relative humidity of the climatic chamber were stabilized at reference values. A random sequence was followed to test the 15 different samples.

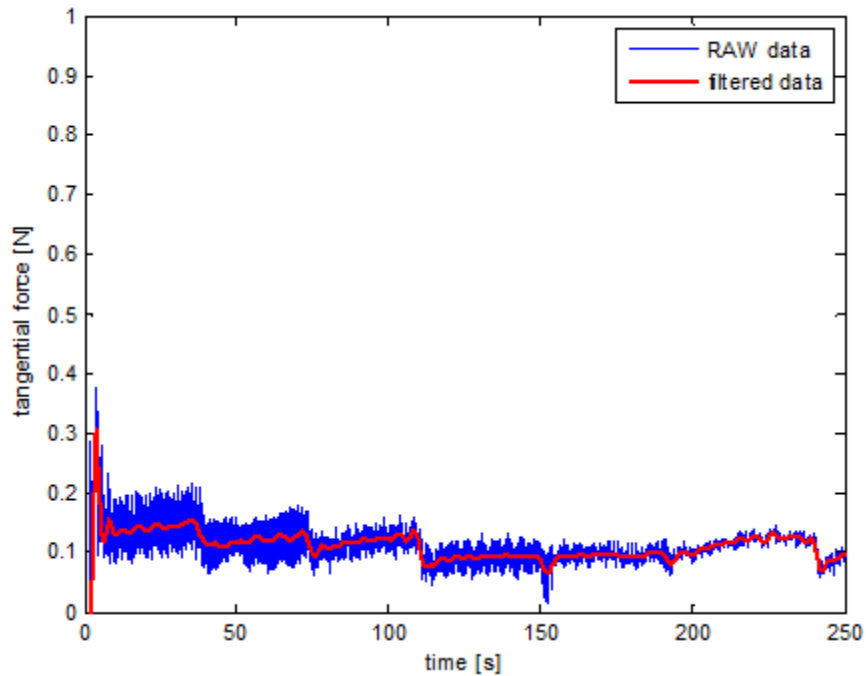


Figure 4 (Color Online) Representative performance test; the step by step speed increases are evident.

III. THE FRICTION MODEL

A. Performance tests

In order to calculate the friction coefficient via tribometer tests, the rotational speed, as imposed to the electric motor, and the friction tangential force, as measured by the load cell, were collected. To analyse the data we use a simple model, based on the equations:

$$\omega = \frac{2 \cdot \pi \cdot rpm}{60} \quad (1)$$

and

$$v = \omega \cdot d \quad (2)$$

where rpm is the rotational speed of electric motor, ω [rad/s] the angular speed of the plate containing the snow, v [m/s] the tangential speed of the sample, d [mm] the distance from the centre of the plate and the centre of the sample (equal to 140 mm). This information allows to calculate the equivalent skier speed (in km/h).

It is now possible to calculate the friction coefficient, considering that the normal force is:

$$F_N = m \cdot g \quad (3)$$

and the tangential force is:

$$F_t = \mu \cdot F_N \quad (4)$$

The mass m [kg] is chosen in order to simulate the average pressure distribution of a real average skier, g is the gravity acceleration (9.81 m/s²), F_N and F_t are measured in N. The dimensionless friction coefficient μ is calculated as:

$$\mu = \frac{F_t}{F_N} \quad (5)$$

Taking a ski, 1700 mm in length with an average width of 85 mm, the contact area of two skis is 289000 mm². Knowing that the area of samples is 2500 mm² and considering the mass of the skier is about 70 kg, it is possible to calculate the equivalent mass value:

$$m = \frac{70 \cdot 2500}{289000} = 0,605 \text{ kg} \quad (6)$$

For each tested condition (see Table 5) and for each speed step, different values of friction coefficient were found. Such values were analysed and the normal distribution was calculated, with the least-squares method. The results were used to determine the best curve, fitting the experimental values with the Stribeck model²⁵:

$$\mu_{stribeck} = \mu_0 + \mu_1 v + \frac{\mu_2}{v} \quad (7)$$

where $\mu_{stribeck}$ is the friction coefficient; μ_0 , μ_1 and μ_2 are constants and v is the changing tested speed.

B. Results and discussion

Figure 5 reports an example of curve fitting on the experimental data obtained for an UHMWPE ski base. The procedure was repeated for all the test conditions (materials, preparation, rotational speed) and the results are summarized in Figure 6.

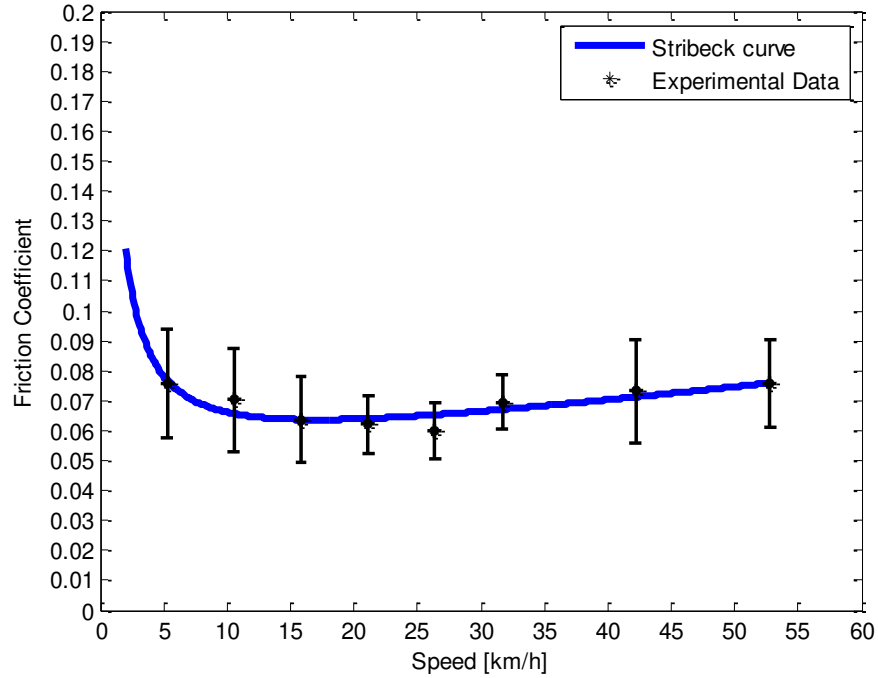


Figure 5 (Color Online) Stribeck curve assessment for UHMWPE sample

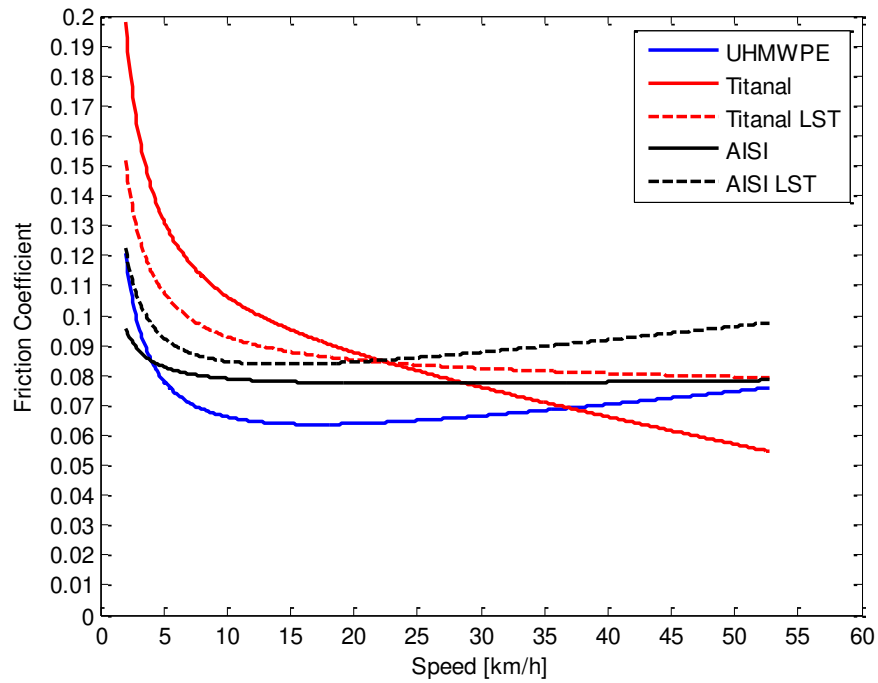


Figure 6 (Color Online) Comparison between gliding performance of the different samples

In Table 7 the coefficients entering for the friction coefficient according to the Stribeck model, see equation (7), for the different tested samples are reported.

Table 7 Coefficients of the Stribeck friction model for each sample

Sample	μ_0	μ_1	μ_2
UHMWPE	0.046	5.06e-4	0.147
AISI 301	0.074	6.97e-5	0.043
AISI 301 LST	0.069	5.01e-4	0.105
Titanal	0.093	-8.09e-4	0.212
Titanal LST	0.079	-4.32e-5	0.146

UHMWPE shows the lowest friction coefficient values, corresponding to the best performance of the ski base at all speeds. The result is not particularly surprising considering that all the tested UHMWPE samples were waxed at the state of the art. On the contrary, no wax-equivalent treatments were applied to metallic samples. This choice was deliberately made to compare metal base performances with the presently available best ones.

Laser treated AISI 301 presents a trend similar to UHMWPE, although with slightly higher μ_0 and μ_1 values (about +25%). The adopted, non-optimized LST affects the metal ski surface at the micron scale and it results in an increase of the apparent contact area between ski and snow. This produces an increase in the number of surface asperities and consequently in the friction coefficient that is not compensated by the concomitant hydrophobicity increase resulting after LST (see Figure 2).

Pristine AISI 301 and laser treated Titanal® display a trend almost independent from speed. Such a behaviour is not surprising, since it was reported for UHMWPE over a wide range of temperatures and speed values², including those explored in the present study. However, at speeds still higher than 55 km/h, it is likely that an inversion with respect to UHMWPE can occur.

Pristine and LST Titanal® present a trend that differs from all the other typologies and shows very high friction coefficient values at low speeds and the lowest values at the highest speeds, thus a negative μ_1 coefficient (see Table 7). This is due to the surface imprinting rather than to LST machining. As a result, the minimum position, typical of Stribeck model of friction²⁵ shifts beyond the upper speed explored in the present study (50-55 km/h).

We recall that UHMWPE and pristine Titanal are the only solutions on which an imprint was applied. The procedure produces an increase in the detachment friction coefficient but it also reduces the friction at higher speeds. This is also the reason of the observed crossover point for the Titanal pristine and LST at mid-low speed (22 km/h). Similarly, the break-even point between UHMWPE and Titanal pristine occurs at mid-high speed (35-40 km/h) while at 50 km/h the improvement is about -30%.

IV. CONCLUSIONS

This work aimed at utilizing different materials in the construction of a ski base. In particular, we focused on metallic materials that show a good gliding behaviour on compact, icy, dry snow. From laboratory tests, it is possible to deduce how two metallic materials, namely AISI 301 stainless steel and an aluminium alloy (Titanal®), behave

similarly to UHMWPE when gliding on such a snow. Both metals show slightly worse gliding at low speeds but have low friction coefficients at high speeds.

The micrometric dimple texture, resulting from laser treatment, despite presents a hydrophobic behaviour on the machined materials, does not improve significantly the performance of both the metals in contact with snow. On Titanal®, Laser Surface Texturing improves the friction coefficient at low speeds, but worsens it at high speeds. On AISI 301 the friction coefficient values are similar in laser treated and pristine samples without any meaningful increase of the performances. A modelling study to optimize the feature size, shape, and spacing is planned for ongoing work. [The present paper underlines the need of this, since the present results indicate that improvements in ski performance are feasible along this path, although performance optimization was beyond the scope of the present research.]

ACKNOWLEDGMENTS

The authors would like to acknowledge Blossom Skis for the technical and financial contribution to this research.

REFERENCES

- 1 A. M. Kietzig, S. G. Hatzikiriakos and P. Englezos, *J. Appl. Phys.* **107**(8), 0-15 (2010).
- 2 L. Makkonen, and M. Tikanmäki, *Cold Reg Sci Technol.* **76-77**, 24-36 (2012).
- 3 L. Baurle, D. Szabò, M. Fauve, H. Rhyner, and N. D. Spencer, *Tribol. Lett.* **24**(1), 77-84 (2006).
- 4 M. Scherge, R. Bottcher, M. Richter and U. Gurgel, *Tribol. Lett.* 1-6 (2012).
- 5 S. Rohm, M. Hasler, C. Knoflach, J. van Putten, S. H. Unterberger, K. Schindelwig, and W. Nachbauer, *Tribol. Lett.* **59**(1), 27 (2015).
- 6 A. M. Kietzig, S. G. Hatzikiriakos and P. Englezos, *J. Appl. Phys.* **106**(2), 1-16 (2009).
- 7 M. Susoff, K. Siegmann, C. Pfaffenroth, and M. Hirayama, *Appl. Surf. Sci.* **282**, 870–879 (2013).
- 8 T. Bharathidasan, S. V. Kumar, M. S. Bobji, R. P. S. Chakradhar, and B. J. Basu, *Appl. Surf. Sci.* **314**, 241-250 (2014).
- 9 A. M. Kietzig, S. G. Hatzikiriakos and P. Englezos, *J. Galciol.* **56**(197), 473-479 (2010).
- 10 A. M. Kietzig, S. G. Hatzikiriakos and P. Englezos, *Langmuir.* **25**(8), 4821-7 (2009).
- 11 P. Bizi-Bandoki, S. Benayoun, S. Valette, B. Beaugiraud, and E. Audouard, *Appl. Surf. Sci.* **257**(12), 5213-5218 (2011).
- 12 A. G. Demir, V. Furlan, N. Lecis, and B. Previtali, *Biointherphases.* **9**(2), 0290091-10 (2014).
- 13 A. B. D. Cassie and S. Baxter, *Trans. Faraday Soc.* **40**, 546 (1944).
- 14 L. O. Andersson, C. G. Golander and S. Persson, *J. Adhes. Sci. Techno.* **8**, 117-132 (1994).
- 15 S. Frankenstein and A.-M. Tuthill, *J. Cold. Reg. Eng.* **16**, 83-96 (2002).
- 16 K. Golovin, S.-P.-R. Kobaku, D. H. Lee, E. T. DiLoreto, J. M. Mabry and A. Tuteja, *Sci. Adv.* **2**, 1501496 (2016).
- 17 S. C. Colbeck, *J. Sports Sci.* **3**(12), 285-295 (1994).
- 18 G. De Koning, G. J. De Groot and J. V. I. Schenau, *J. Biomech.* **25**(6), 565-571 (1992).

- ¹⁹I. Etsion, *J. Tribol.* **127**, 248-253 (2005).
- ²⁰A. Erdemir, *Tribol. Internat.* **38**, 249-256 (2005).
- ²¹H. Yu, X. Wang and F. Zhou, *Tribol. Lett.* **37**(2), 123-130 (2010).
- ²²P. Maressa, L. Anodio, A. Bernasconi, A. G. Demir and B. Previtali, *J. Adhes.* **91**(7), 518-537 (2015).
- ²³A. G. Demir, B. Previtali, and N. Lecis, *Opt. Laser Technol.* **54**, 53-61 (2013).
- ²⁴ASTM D7334. Standard Practice for Surface Wettability of Coatings, Substrates and Pigments by Advancing Contact Angle Measurement1, D7334 – 08 (2013).
- ²⁵H. Czichos and K. H. Habig, *Tribologie-Handbuch (Tribology handbook)*, (Vieweg Verlag, Wiesbaden, 2nd edition, 2003).